Environ Sci Pollut Res
DOI 10.1007/s11356-017-9956-7

RESEARCH ARTICLE

Performance, emission, and combustion characteristics of twin-cylinder common rail diesel engine fuelled with butanol-diesel blends

Venkatesh Tavareppa Lamani[1] · **Ajay Kumar Yadav**[1] · **Kumar Narayanappa Gottekere**[1]

Received: 13 March 2017 / Accepted: 11 August 2017

Abstract Nitrogen oxides and smoke are the substantial emissions for the diesel engines. Fuels comprising high-level oxygen content can have low smoke emission due to better oxidation of soot. The objective of the paper is to assess the potential to employ oxygenated fuel, i.e., n-butanol and its blends with the neat diesel from 0 to 30% by volume. The experimental and computational fluid dynamic (CFD) simulation is carried out to estimate the performance, combustion, and exhaust emission characteristics of n-butanol-diesel blends for various injection timings (9°, 12°, 15°, and 18°) using modern twin-cylinder, four-stroke, common rail direct injection (CRDI) engine. Experimental results reveal the increase in brake thermal efficiency (BTE) by ~ 4.5, 6, and 8% for butanol-diesel blends of 10% (Bu10), 20% (Bu20), and 30% (Bu30), respectively, compared to neat diesel (Bu0). Maximum BTE for Bu0 is 38.4%, which is obtained at 12° BTDC; however, for Bu10, Bu20 and Bu30 are 40.19, 40.9, and 41.7%, which are obtained at 15° BTDC, respectively. Higher flame speed of n-butanol-diesel blends burn a large amount of fuel in the premixed phase, which improves the combustion as well as emission characteristics. CFD and experimental results are compared and validated for all fuel blends for in-cylinder pressure and nitrogen oxides (NO_x), and found to be in good agreement. Both experimental and simulation results witnessed in reduction of smoke opacity, NO_x, and carbon monoxide emissions with the increasing n-butanol percentage in diesel fuel.

Keywords CRDI · Combustion analysis · Biofuel · Emission · Butanol · CFD

Nomenclature

ATDC	After top dead center
Bu	Butanol
CRDI	Common rail direct injection
D_t	Diffusion coefficient
$\widetilde{E}_{Fu}^{F\to M}$	Unmixed fuel source term
$\widetilde{E}_{O_2}^{A\to M}$	Unmixed oxygen source term
ECFM3Z	Extended coherent flame model three zone
EVC	Exhaust valve closing
EVO	Exhaust valve opening
IMAP	Intake manifold air pressure
IMAT	Intake manifold air temperature
IT	Injection timing
IVO	Inlet valve opening
IVC	Inlet valve closing
M_{Fu}	Molar mass of fuel
R	Universal gas constant
S_c and S_{ct}	Laminar and turbulent Schmidt numbers
$\overline{S}_{NO}$	Mean nitric oxide source term
$\tilde{u}$	Density-weighted average velocity
$\overline{\dot{\omega}}_x$	Average combustion source term

Greek letters

ζ	Transformed coordinate system
$\overline{\rho}^u\vert_u$	Density of the unburned gases
ε	Dissipation rate
ϕ	Equivalence ratio
ϕ_s	Soot mass fraction

Responsible editor: Philippe Garrigues

✉ Ajay Kumar Yadav
ajayyadav.aba@rediffmail.com

[1] Department of Mechanical Engineering, National Institute of Technology Karnataka, Surathkal, Mangalore 575 025, India

Published online: 25 August 2017

μ	Dynamic viscosity
τ_d	Ignition delay
$\overline{\rho}$	Reynolds averaged fuel density
$\tilde{Y}_{NO}$	Mean mass fraction of NO_x
x_i	Cartesian coordinates
M_{NO}	Molar mass
$\frac{dc_{NO\ prompt}}{dt}$	Prompt mechanisms
$\frac{dc_{NO\ thermal}}{dt}$	Thermal mechanisms
μ_t	Turbulent viscosity
$\tilde{Y}_x$	Averaged mass fraction of species x
M^M	Mean molar mass of the gases in the mixed area
M_{Fu}	Molar mass of fuel
$M_{air+EGR}$	Mean molar mass of the unmixed air + EGR gases
$\overline{\rho}$	Mean density
$\tilde{Y}_{O_2}^{\infty}$	Oxygen mass fraction
τ_m	Mixing time
$\tilde{Y}_{TO_2}$	Oxygen tracer
$\tilde{Y}_{TFu}$	Fuel tracer

Introduction

The depletion of fossil fuels is one of the major problems the world is facing today. Searching for alternative fuels has gained a lot of importance in the recent past of which biodiesel and alcohols are widely tested. Due to high density and viscosity, biodiesel limits its usage in CI engines as it results in poor atomization. On the other hand, alcohol is a renewable fuel as it can be produced from biomass (Atmanli et al. 2015). It is also an oxygenated fuel which further helps in reduction of soot (Lamani et al. 2017a).

This research work uses n-butanol over methanol and ethanol because of its higher cetane number (Ibrahim 2016) and approximately 25% more energy content (Chen et al. 2014). Butanol has a higher heat of evaporation compared to ethanol resulting in reduced combustion temperature which might be the possible reason for reduction in NO_x (Dernotte et al. 2010). Chotwichien et al. (2009) showed that butanol-diesel blends are more suitable for CI engines as compared to ethanol-diesel blends owing to their better solubility in the diesel fuel. Various experimental investigations are carried out to study the effect of butanol-diesel blend on performance and tail pipe emissions of CI engines. Rakopoulos et al. (2010a, b) observed reduction in CO, NO_x, and smoke density with increase in blend ratio; on contrary, HC emissions increased. Chen et al. (2013) obtained an increase in thermal efficiency as well as specific fuel consumption with increasing blend ratios. Doğan (2011) also reported similar results of increase in brake thermal efficiency (BTE), specific fuel consumption (SFC), and hydrocarbon along with decrease in NO_x, CO, and smoke opacity with increasing butanol-diesel blend ratio. Choi et al. (2015) and Jin et al. (2011) achieved a significant drop (50–73%) in particulate matter and soot, respectively, with n-butanol diesel blends. Miers et al. (2008) also reported 80% reduction in smoke for 40% butanol blend without much increase in NO_x emissions. da Silva Trindade and dos Santos (2017) reported that the use of butanol diesel blends has a positive effect on the emission characteristics. Moreover, Campos-Fernández et al. (2012) concluded that 30% butanol-diesel blend might replace the use of pure diesel in CI engines without any engine modification and without any significant loss in performance. Zhang et al. (2012), Zhang and Balasubramanian (2014), and Siwale et al. (2013) also observed similar results.

In addition to find an alternative fuel, operating parameters are required to be optimized to get better performance with alternative fuels without any modification in existing engine. There is limited literature available on the optimization of injection timing for butanol-diesel blends, and hence, this research work aims to optimize this important parameter. In present study, optimum injection timings are obtained for different butanol-diesel blends (Bu0, Bu10, Bu20, and Bu30) experimentally to get maximum brake thermal efficiency. Tailpipe emissions (NO_x, CO, and soot) at various injection timings (9°, 12°, 15°, and 18°) are also measured for the butanol-diesel blends. Trade-off can be obtained based on BTE and exhaust emissions. Further, CFD simulation is carried out for all injection timings and butanol-diesel blends considered for experimental studies. In-cylinder temperature variation for various injection timings is portrayed in form of contour plots which gives the realistic visualization of combustion phenomenon for neat diesel as well as for butanol-diesel blends. An appropriate combustion model is proposed for butanol-diesel blends which may be suitable for similar fuels. Such numerical and experimental studies are not available in open literature.

Fuel properties and combustion strategy

Fuel preparation

In present investigation, n-butanol-diesel blends are considered for numerical and experimental studies. The n-butanol is blended with the neat diesel to obtain different blends of n-butanol-diesel blends from 0 to 30% by volume. Bu0, Bu10, Bu20, and Bu30 represent 0, 10, 20, and 30% n-butanol in neat diesel. Furthermore, stability analysis of n-butanol blends is carried out by observing the blend phase for 6 months; blends remained stable without phase separation as shown in Fig. 1. Basic physical properties of the n-butanol and neat diesel employed in this investigation are compared in Table 1 (Rakopoulos et al. 2010a, b), and range of experimental parameters are listed in Table 2.

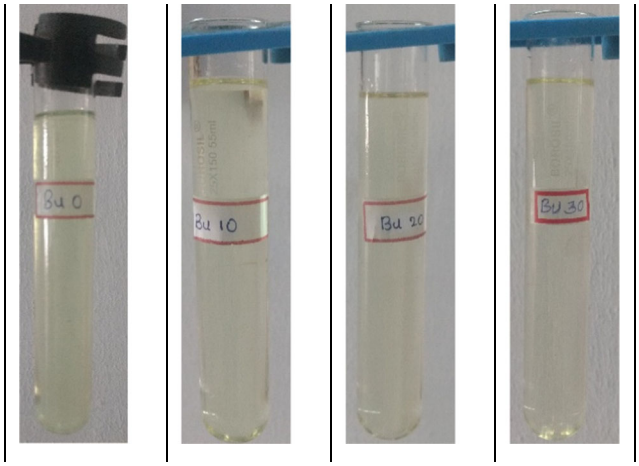

Fig. 1 Stability analysis of n-butanol blends

Table 1 Properties of diesel and n-butanol

Fuel properties	Diesel	n-Butanol
Density at 20 °C (kg/m^3)	837	810
Cetane number	50	25
Lower calorific value (MJ/kg)	43	33.1
Kinematic viscosity at 40 °C (mm^2/s)	2.6	3.6
Boiling point (°C)	180–360	118
Latent heat of evaporation (kJ/kg)	250	585
Oxygen (% weight)	0	21.6
Bulk modulus of elasticity (bar)	16,000	15,000
Stoichiometric air–fuel ratio	15	11.2
Molecular weight	170	74

Source: Rakopoulos et al. (2010a, b)

Experimental setup

Schematic diagram and representation of experimental facility are shown in Fig. 2a, b. Twin cylinder, CRDI engine with open electronic control unit (ECU) developed by *NIRA Control AB*, is used to study the engine performance, emission, and combustion characteristics. The specifications of the engine are listed in Table 3.

The fuel from the tank is supplied to the accumulator (common rail) by high-pressure fuel pump at constant injection pressure of 100 MPa. Common rail pressure is maintained by pressure control valve (PCV), and required fuel supplied to injector is controlled by solenoid valve. Operating parameters of engine are controlled by an open ECU developed by *NIRA Control AB*. Pressure versus crank angle data is measured by using piezo-electric-based pressure transducer. The signal of cylinder pressure is acquired at every 1° crank angle for 100 cycles, and average value of 100 cycles is considered for combustion analysis. The pressure signal is fed into the NI USB-6210 DAQ, then to a data acquisition card linked to the computer. Further engine tail pipe emissions are measured by exhaust gas analyzer (AVL 444) with diesel probe to measure the concentrations of HC, CO, NO, CO_2, and O_2. The details of the engine instrumentation and range are presented in Tables 4 and 5. Soot emission is measured by opacity meter (AVL 415SE).

Error analysis

Assessment of uncertainties and error is necessary while conducting any experimental study. Uncertainties may appear because of numerous reasons like environmental conditions, calibration, observation, instrument selection, and incorrect reading. Error analysis quantifies the accuracy of the experiments being performed. The uncertainties of dependent parameters like brake power and fuel consumption are computed by partial differentiation method using the uncertainty percentages of various instruments as shown in Table 5. The uncertainties for independent parameters were found by calculating the mean, standard deviation, and standard error for the repeated set of 20 readings. The total uncertainty of the experimental investigation is

$$= \text{Square root of} \left\{ \begin{array}{l} (\text{uncertainty of CO})^2 + (\text{uncertainty of NO})^2 + (\text{uncertainty of soot})^2 + (\text{uncertainty of load})^2 \\ + (\text{uncertainty of speed})^2 + (\text{uncertainty of time})^2 + (\text{uncertainty of brake power})^2 \\ + (\text{uncertainty of fuel consumption})^2 + (\text{uncertainty of brake thermal efficiency})^2 \\ + (\text{uncertainty of cylinder pressure})^2 + (\text{uncertainty of crank angle})^2 + (\text{uncertainty of manometer})^2 \end{array} \right\}$$

$$= \text{Square root of} \left\{ (0.1)^2 + (0.6)^2 + (0.1)^2 + (1.3)^2 + (0.1)^2 + (0.2)^2 + (0.8)^2 + (0.2)^2 + (0.8)^2 + (0.9)^2 + (0.1)^2 + (0.2)^2 \right\} \pm 2.076\%$$

Table 2 Range of simulation parameters

Parameters	Range
Blend (percent of butanol)	0, 10, 20, and 30
Injection timings (BTDC)	9°, 12°, 15°, and 18°

Table 3 Engine specifications

Make	Mahindra Maximmo
Number of cylinders	2
Bore × stroke (mm)	83 × 84
Connecting rod length (mm)	141
Swept volume (cm^3)	909
Compression ratio	18.5
Injection type	Common rail
Injection pressure (MPa)	100

CFD code and meshing of geometry

AVL ESE CFD tool is used for engine geometric modeling and computational meshing as shown in Fig. 3. The injector with seven holes is located centrally on the top of piston; hence, 52° sector is chosen for the simulation. In order to reduce the computational time, high-pressure cycle is considered. Simulation is started and ended at inlet valve close and exhaust valve open position, respectively. Grid independence test has been carried out to obtain optimum grid size as shown in Fig. 4. Simulation is carried out by 64-GB RAM 32 core workstation with parallel processing. Results have been checked for peak pressure and computational time for various grid sizes. It has been observed that considered parameters are invariant with change in total number of grids at/after 3×10^5. Boundary conditions and models employed in the simulation are listed in Tables 6 and 7, respectively.

Governing equations

A general transport equation for chemical species is given by (Kuo 1986).

$$\frac{\partial\left(\overline{\rho}\tilde{Y}_x\right)}{\partial t}+\frac{\partial\left(\overline{u}_i\overline{\rho}\tilde{Y}_x\right)}{\partial x_i}=\frac{\partial}{\partial x_i}\left(\left(\frac{\mu}{S_c}+\frac{\mu}{S_{ct}}\right)\frac{\partial\tilde{Y}_x}{\partial x_i}\right)+\overline{\dot{\omega}}_x \quad (1)$$

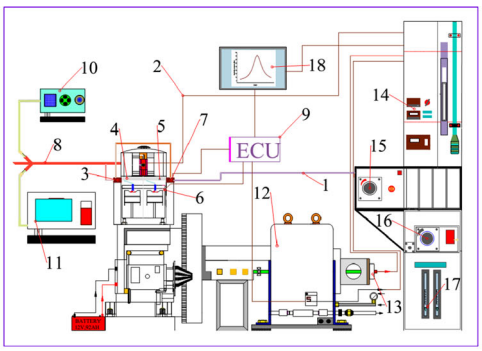

(a)

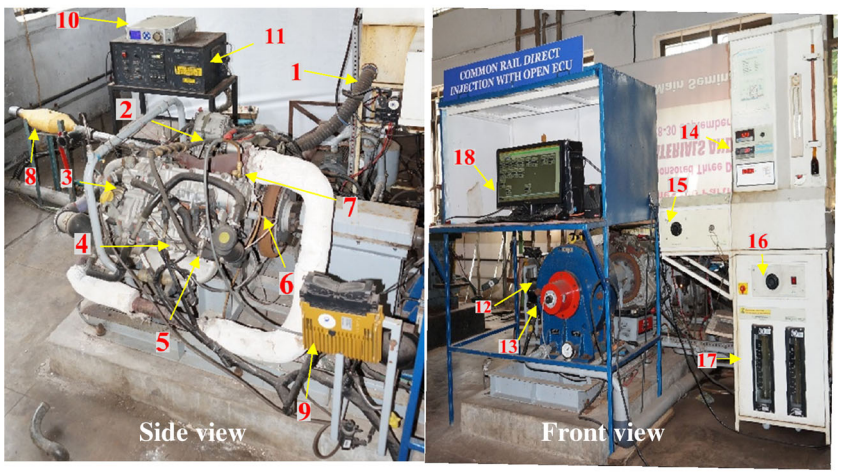

(b)

Fig. 2 **a** Schematic diagram. **b** Experimental facility. 1. Airline, 2. Fuel line, 3. EGR Valve, 4. Common Rail, 5. Pressure control valve, 6. Pressure transducer, 7. Vacuum pump, 8. Exhaust line, 9. ECU, 10. Gas analyzer, 11.Smoke meter, 12. Dynamometer, 13. Encoder, 14. Speed and load display unit, 15. Throttle control unit, 16. Load control unit, 17. Rota meters, 18. Computer display

Table 4 Details of the engine instrumentations

Instrument	Functional use	Measuring technique
i. Saj test. eddy dynamometer	Load	Load cell
ii. PCB piezotronics, pressure transducer	Pressure	Piezo-electric sensor
iii. Piezo-charge amplifier	A/D converter	Piezo-electric sensor
iv. Angle encoder	Crank angle	Magnetic pickup type
v. AVL Di-Gas 444 exhaust gas analyzer	NO_x	Chemiluminescence detector (CLD)
	CO	Non-dispersive infrared (NDIR)
	HC emissions	Flame ionization detector (FID)
vi. AVL 415SE	Soot	Opacity

Fuel transport equations for unburned and burned fuel mass fractions are given by FIRE v2011 Manuals (2011) and Colin and Benkenida (2004).

$$\frac{\partial\left(\overline{\rho}\tilde{Y}^{u}_{Fu}\right)}{\partial t}+\frac{\partial\left(\overline{\rho}\tilde{u}_i\tilde{\bar{Y}}^{u}_{Fu}\right)}{\partial x_i}=\frac{\partial}{\partial x_i}\left(\left(\frac{\mu}{S_c}+\frac{\mu_t}{S_{ct}}\right)\frac{\partial\tilde{Y}^{u}_{Fu}}{\partial x_i}\right)+\overline{\rho}\tilde{S}^{u}_{Fu}+\bar{\dot{\omega}}^{u}_{Fu}+\bar{\dot{\omega}}^{u\to b}_{Fu} \quad (2)$$

$$\frac{\partial\left(\overline{\rho}\tilde{Y}^{b}_{Fu}\right)}{\partial t}+\frac{\partial\left(\overline{\rho}\tilde{u}_i\tilde{Y}^{b}_{Fu}\right)}{\partial x_i}=\frac{\partial}{\partial x_i}\left(\left(\frac{\mu}{S_c}+\frac{\mu_t}{S_{ct}}\right)\frac{\partial\tilde{Y}^{b}_{Fu}}{\partial x_i}\right)+\overline{\rho}\tilde{S}^{b}_{Fu}+\bar{\dot{\omega}}^{b}_{Fu}+\bar{\dot{\omega}}^{u\to b}_{Fu} \quad (3)$$

The equations for unmixed species, i.e., fuel and air are

$$\frac{\partial\left(\overline{\rho}\tilde{Y}^{F}_{Fu}\right)}{\partial t}+\frac{\partial\left(\overline{\rho}\tilde{u}_i\tilde{Y}^{F}_{Fu}\right)}{\partial x_i}-\frac{\partial}{\partial x_i}\left(\left(\frac{\mu}{S_c}+\frac{\mu_t}{S_{ct}}\right)\frac{\partial\tilde{Y}^{F}_{Fu}}{\partial x_i}\right)=\overline{\rho}\tilde{S}^{F}_{Fu}+\overline{\rho}\tilde{E}^{F\to M}_{Fu} \quad (4)$$

$$\frac{\partial\left(\overline{\rho}\tilde{Y}^{A}_{O_2}\right)}{\partial t}+\frac{\partial\left(\overline{\rho}\tilde{u}_i\tilde{Y}^{A}_{O_2}\right)}{\partial x_i}-\frac{\partial}{\partial x_i}\left(\left(\frac{\mu}{S_c}+\frac{\mu_t}{S_{ct}}\right)\frac{\partial\tilde{Y}^{A}_{O_2}}{\partial x_i}\right)=\overline{\rho}\tilde{E}^{A\to M}_{O_2} \quad (5)$$

The amount of mixing is computed with a characteristic timescale based on the k-ε model.

$$\overline{E}^{F\to M}_{Fu}=-\frac{1}{\tau_m}\tilde{Y}^{F}_{Fu}\left(1-\tilde{Y}^{F}_{Fu}\frac{\overline{\rho}M^{M}}{\overline{\rho}^{u}\left|_{u}M^{u}{}_{Fu}\right.}\right) \quad (6)$$

$$\overline{E}^{A\to M}_{O_2}=-\frac{1}{\tau_m}\tilde{Y}^{A}_{O_2}\left(1-\frac{\tilde{Y}^{A}_{O_2}}{\tilde{Y}^{\infty}_{O_2}}\frac{\overline{\rho}M^{M}}{\overline{\rho}^{u}\left|_{u}M^{u}{}_{\text{air + EGR}}\right.}\right) \quad (7)$$

where τ_m is the mixing time defined as

$$\tau_m^{-1}=\frac{\varepsilon}{k} \quad (8)$$

The oxygen mass fraction in unmixed air is computed as follows:

$$\tilde{Y}^{\infty}_{O_2}=\frac{\tilde{Y}_{TO_2}}{1-\tilde{Y}_{TFu}} \quad (9)$$

Pollutant model

The transport equation model for nitrogen monoxide is given by (Petranovic et al. 2015; Heywood 1988)

$$\frac{\partial\left(\overline{\rho}\tilde{Y}_{NO}\right)}{\partial t}+\frac{\partial\left(\overline{u}_i\overline{\rho}\tilde{Y}_{\text{NO}}\right)}{\partial x_i}=\frac{\partial}{\partial x_i}\left(\overline{\rho}D_t\frac{\partial\tilde{Y}_{\text{NO}}}{\partial x_i}\right)+\overline{S}_{\text{NO}} \quad (10)$$

Table 5 Operating range with percentage of uncertainties of instruments used during experiments

Instrument	Measured quantity	Range	Uncertainties (%)
i. Dynamometer	Load	0–50 kg	0.1
ii. AVL Di-Gas 444 analyzer	NO_x	0–5000 ppm	0.1
	CO	0–10 vol.%	0.1
iii. Smoke opacimeter	Smoke opacity	0–100%	1.7
iv. Speed measuring unit	Engine speed	0–9999 rpm	0.1
v. Pressure transducer	Cylinder pressure	0–345 bar	0.1
vi. Crank angle encoder	Crank angle	0–360°	0.2

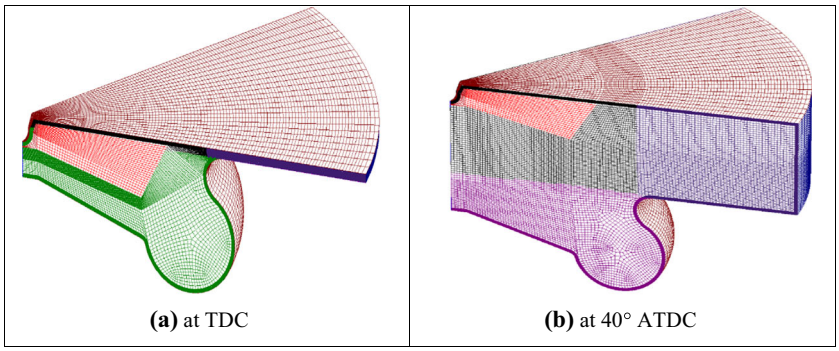

(a) at TDC

(b) at 40° ATDC

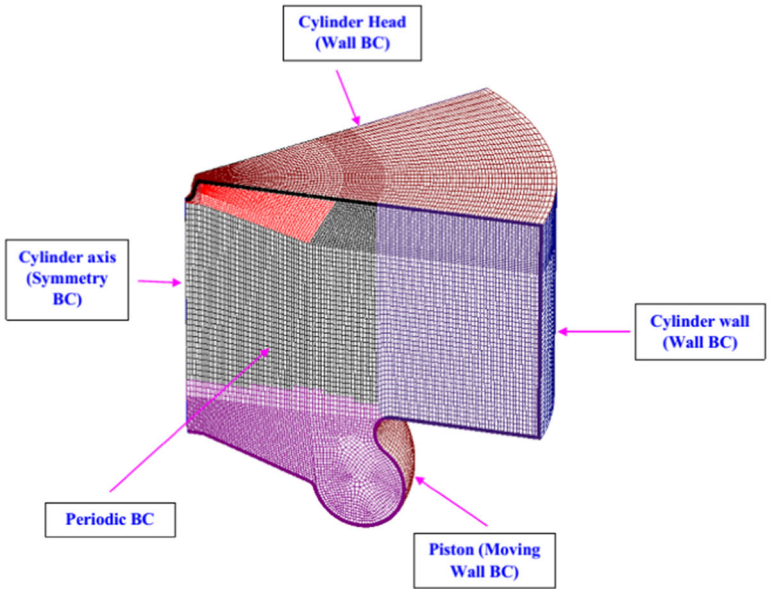

(c) Boundary conditions

Fig. 3 Three-dimensional computational domain

The term $\overline{S}_{NO}$ represents source term for NO formation in the equation.

$$\overline{S}_{NO} = M_{NO}\left(\frac{dc_{NO\ thermal}}{dt} + \frac{dc_{NO\ prompt}}{dt}\right) \tag{11}$$

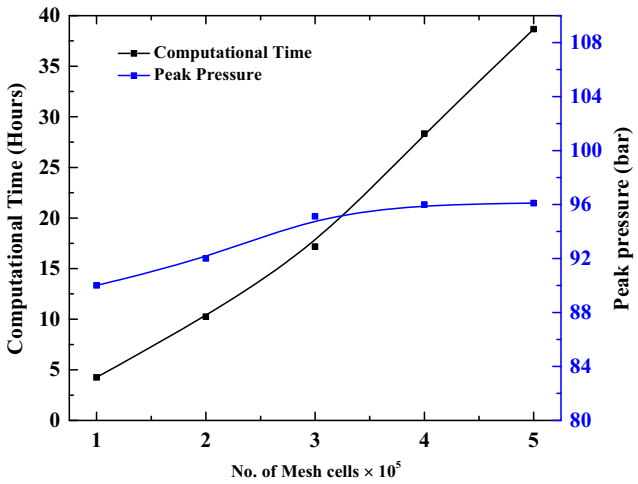

Fig. 4 Grid independence study of peak pressure

The transport equation model for formation mass fraction ϕ_s is given by

$$\frac{\partial}{\partial t}\left(\overline{\rho}\tilde{\phi}_s\right) + \frac{\partial}{\partial x_j}\left(\overline{\rho}\overline{u}_j\overline{\phi}_s\right) = \frac{\partial}{\partial x_j}\left(\frac{\mu_{eff}}{\sigma_s}\frac{\partial\overline{\phi}_s}{\partial x_j}\right) + S_{\varphi_s} \tag{12}$$

Soot formation rate is defined as

$$S_{\varphi_s} = S_n + S_g + S_{O_2} \tag{13}$$

where S_n is the soot nucleation, S_g is the soot growth, and S_{O_2} is the soot oxidation.

Table 6 Calculation domain boundaries

Boundary type	Boundary condition	Values
Piston	Moving mesh	Temperature 570 K
Axis	Periodic inlet/outlet	Periodic
Cylinder head	Wall	Temperature 570 K
Compensation volume	Wall	Thermal/adiabatic boundary
Liner	Wall	Temperature 470 K

Table 7 Models employed for simulation

Model	Options
Turbulence model	*k-ζ-f* model
Breakup model	Wave
Turbulent dispersion model	Enable
Wall treatment	Hybrid wall treatment
Wall impingement model	Walljet 1
Heat transfer wall model	Standard wall function
Evaporation model	Dukowicz and multicomponent model
Combustion model	CFM
Ignition model	ECFM-3Z
Soot formation and oxidation	Kinetic model
NO_x mechanism	Extended Zeldovich
Chemistry solver	Fire internal chemistry interpreter (CHEMKIN II)

Results and discussion

In this section, results of experimental and numerical (CFD) studies on CRDI engine are presented. Results are obtained for n-butanol-diesel blends for various injection timings (9°, 12°, 15°, and 18°).

Effect of various butanol-diesel blends and injection timing on BTE

The influence of injection timing and n-butanol-diesel blend ratio on BTE of CRDI engine is shown in Fig. 5. Results show that there is a significant increase in BTE for all butanol-diesel blends at all injection timings compared to Bu0. This can be attributed to the prompt premixed combustion part possessed by butanol blends, enhanced mixing during ignition delay, oxygen enrichment leading to leaner combustion, and less heat loss (Hulwan and Joshi 2011; Hansen et al. 1989). The enhancement of diffusive combustion is obtained due to oxygen-enriched blends, and hence, the total combustion duration is shortened. The increase in BTE with butanol blends is also ascribed to its higher burning velocity of 45 cm/s (Sarathy et al. 2009) as compared to 33 cm/s for diesel (Sayin 2010). The BTE is increased by ~ 4.5, 6, and 8% for Bu10, Bu20, and Bu30, respectively, compared to Bu0. Optimum BTE obtained for Bu0 is 38.4% at 12° BTDC, while for Bu10, Bu20, and Bu30 are 40.19, 40.9, and 41.7%, respectively, at a common injection timing of 15° BTDC. Doğan (2011), Lamani et al. (2017b), and Rakopoulos et al. (2011) also observed a slight increase in BTE with increasing butanol blend ratio.

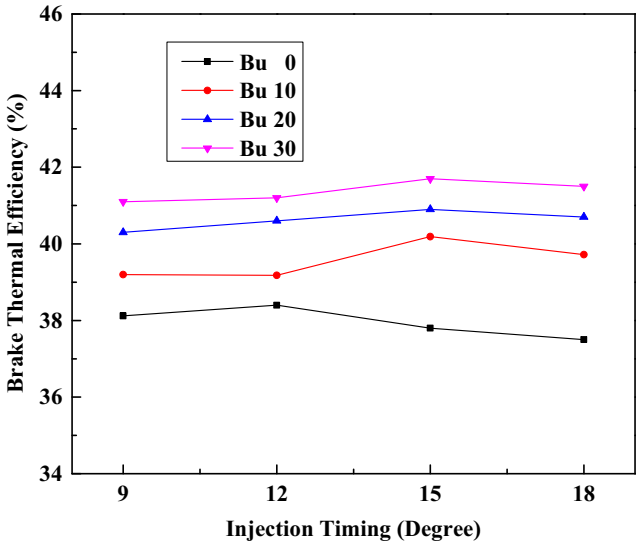

Fig. 5 Variation of brake thermal efficiency versus injection timing

Validation of CFD results with experimental data

In the present study, the engine simulation software AVL-FIRE is coupled with CHEMKIN II for simulating the engine combustion and emission formation processes with detailed reaction mechanisms. The simulation results are validated with the experimental data obtained for conditions listed in Table 2.

Figures 6 and 7 show the comparison of experimental and numerical results of in-cylinder pressure and NO_x emission versus crank angle for neat diesel and blends, respectively. For all validation cases, experimental and CFD results are showing good agreement. It can be seen from the results that peak cylinder pressure slightly increases for butanol blends. This may be because of enhanced premixed combustion phase due to extended ignition delay (Kumar and Saravanan 2016). Results are presented for in-cylinder pressure obtained at 12° BTDC (optimum IT) for Bu0, and 15° BTDC (optimum IT) for Bu10, Bu20, and Bu30 blend ratios, respectively.

Effect of various butanol-diesel blends and injection timings on temperature

The influence of injection timing and n-butanol-diesel blend ratio on in-cylinder temperature of CRDI engine is shown in Fig. 8a–c. Temperature contours (Fig. 8a, b) are plotted for optimum injection timing, i.e., 12° BTDC for neat diesel and 15° BTDC for n-butanol-diesel blends (Bu10, Bu20, and Bu30) at various crank angle (at injection timing, at TDC, and 10° ATDC). Contour plot for Bu0 at 15° BTDC IT is also provided to compare in-cylinder temperature with same IT cases for blends. These contour plots show the clear picture of combustion process occurring inside the cylinder. The temperature contours offer an opportunity to achieve a deeper insight into in-cylinder temperature distribution of n-butanol-diesel blend combustion. Figure 8c represents average in-

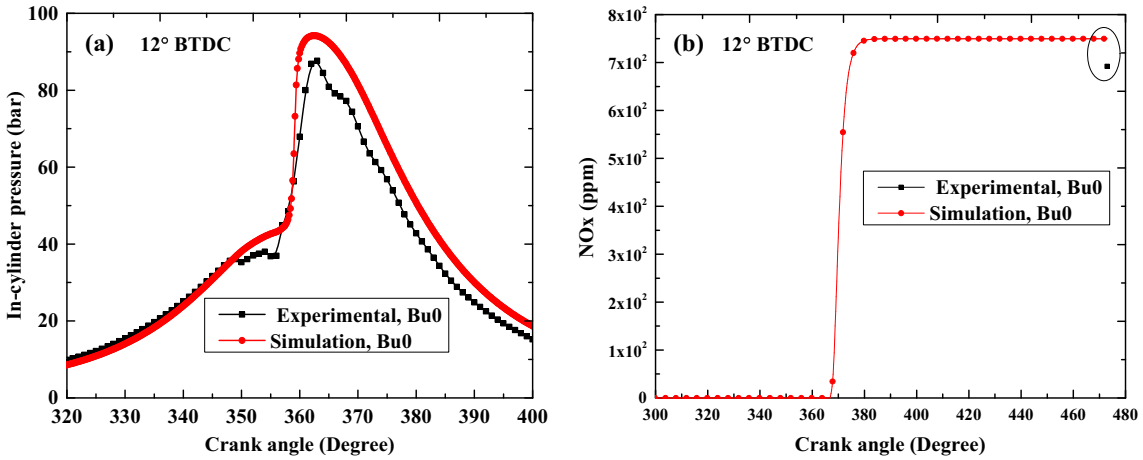

Fig. 6 Validation with experimental results, diesel. **a** In-cylinder pressure versus crank angle. **b** NO_x versus crank angle

cylinder temperature for neat diesel and n-butanol-diesel blends at optimum IT. Results for Bu0 at 15° BTDC IT are also provided to compare in-cylinder temperature with same IT cases for blends. Results show that at same IT, in-cylinder temperature for Bu0 is higher than n-butanol-diesel blend cases, which occurs due to high latent heat of vaporization of n-butanol fuel compared to diesel. At optimum IT, in-cylinder temperature for Bu0 is less than the blends. This occurs due to advance IT for n-butanol-diesel blends compared to neat diesel.

Effect of various butanol-diesel blends and injection timings on NO_x

The oxides of nitrogen in the exhaust emissions contain nitric oxides (NO) and nitrogen dioxides (NO_2). The effect of injection timings and n-butanol-diesel blends on NO_x emission of CRDI engine is shown in Fig. 9a, b. It can be observed from experimental as well as simulation results that NO_x emission tends to decrease with increasing blend concentration. Low cetane number of n-butanol and high heat of evaporation result in a lower flame temperature leads to less NO_x formation compared to neat diesel (Doğan 2011). Also, the amount of NO_x increases with advancement in injection timings as the fuel air mixture gets enough residence time for proper homogeneous mixing. The maximum NO_x emission is 1090, 1001, 989, and 959 ppm for Bu0, Bu10, Bu20, and Bu30, respectively, measured experimentally at 18° BTDC. Obtained numerical results with proposed CFD model show good agreement with experimental data.

Effect of various butanol-diesel blends and injection timing on CO emissions

The effect of injection timing and n-butanol-diesel blend ratio on carbon monoxide (CO) emission of CRDI engine is shown in Fig. 10. CO is formed because of incomplete combustion occurring due to lack of free oxygen during combustion. Since butanol blends are oxygenated, they promote CO oxidation, thereby enhancing the complete combustion process.

As injection timing retards, CO emission increases because of incomplete oxidation taking place during the expansion

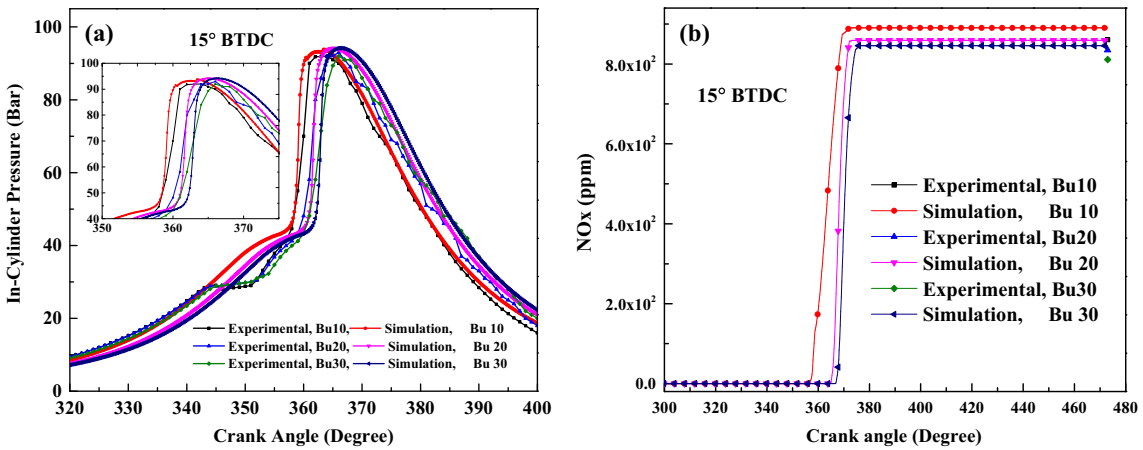

Fig. 7 Validation with experimental results, butanol-diesel blends. **a** In-cylinder pressure versus crank angle. **b** NO_x versus crank angle

stroke. CO emissions are found to be decreased with increasing blend ratio at all injection timings. Advance injection timing leads to early start of combustion causing higher cylinder temperature results in quick chemical reaction between carbon and oxygen in the combustion chamber which intensifies the oxidation process (Sayin et al. 2008). Obtained numerical results with proposed CFD model show marginal difference with experimental data.

Effect of various butanol-diesel blends and injection timing on soot opacity emissions

The particulate matter (PM) is basically composed of soot and is accountable for the smoke. Smoke opacity formation ensues at the air deficit conditions which locally exist in engine cylinder and increases as the air/fuel ratio declines. Soot is formed by poor oxygen thermal cracking of long-chain

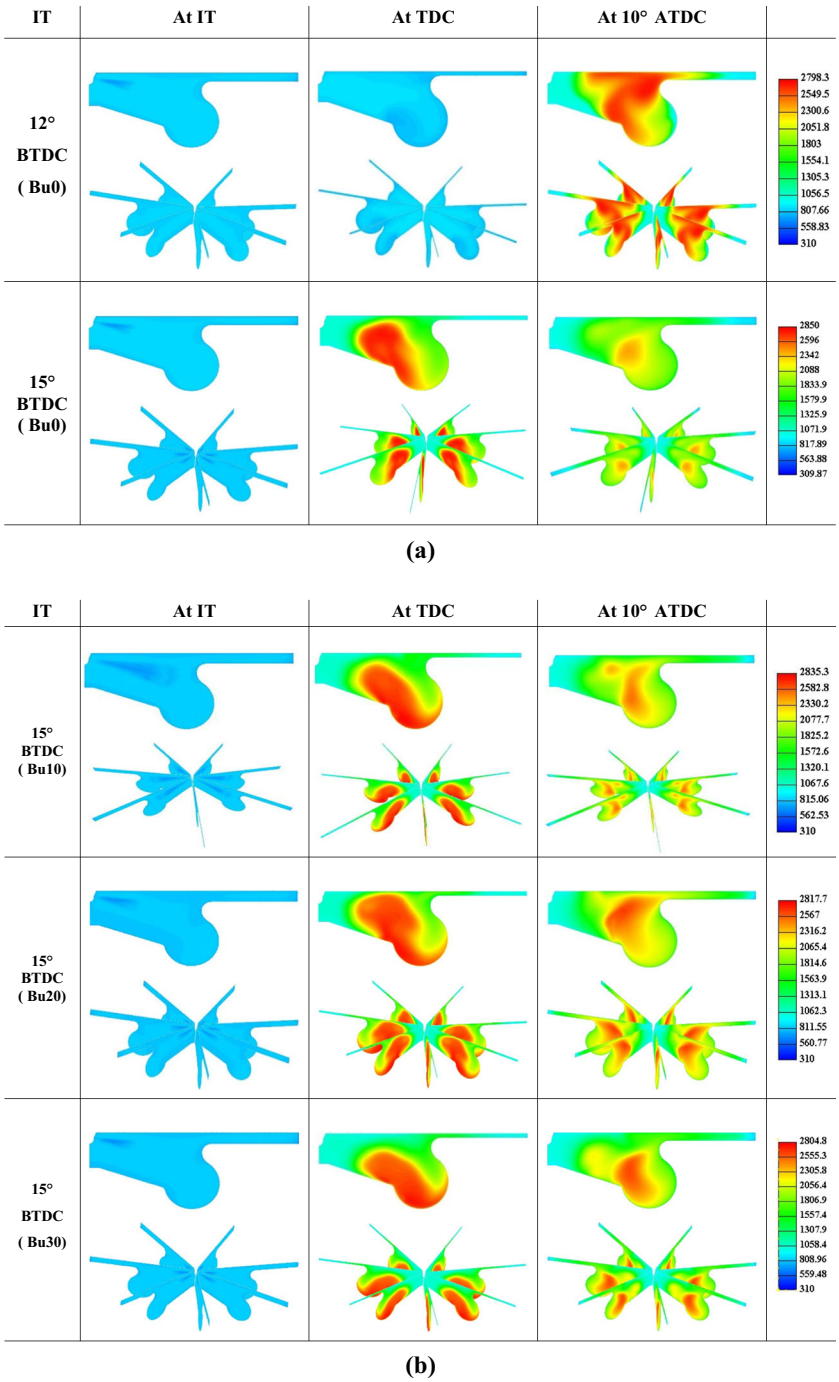

Fig. 8 **a** Temperature contours for diesel. **b** Temperature contour for n-butanol-diesel blends. **c** Temperature versus injection timings

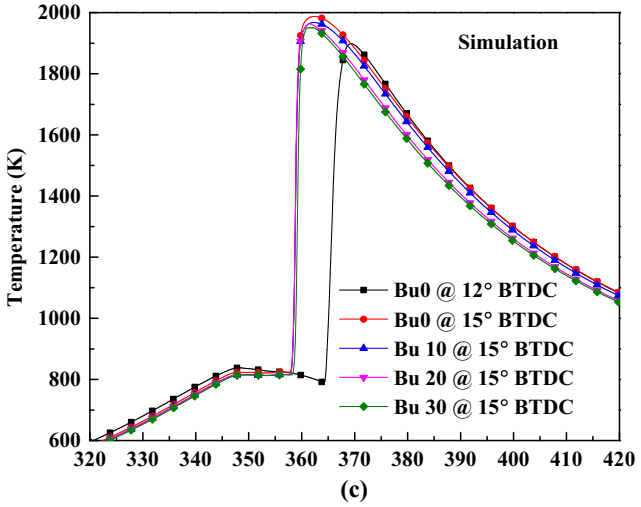

Fig. 8 continued.

molecules (Schobert 2013). The effect of injection timing and n-butanol-diesel blend ratio on soot opacity emission of CRDI engine is studied experimentally as well as numerically and presented in Fig. 11a, b, respectively. Increasing butanol content in the blends results in the reduction of soot due to higher oxygen/carbon ratio.

The existence of atomic oxygen bond in butanol fulfills progressive chemical control over soot formation. The ability to produce soot by the densed fuel region inside a blend diffusion flame sheath gets reduced due to improved mixing owing to better atomization and vaporization of blends. Higher soot formation with retardation in injection timing occurs due to low in-cylinder temperature which weakens soot oxidation. Maximum soot opacity for Bu0, Bu10, Bu20, and Bu30 are 0.042, 0.04, 0.035, and 0.032 measured at 9° BTDC, respectively. Smoke meter used for present experimental studies measures soot opacity instead of soot mass fraction. CFD

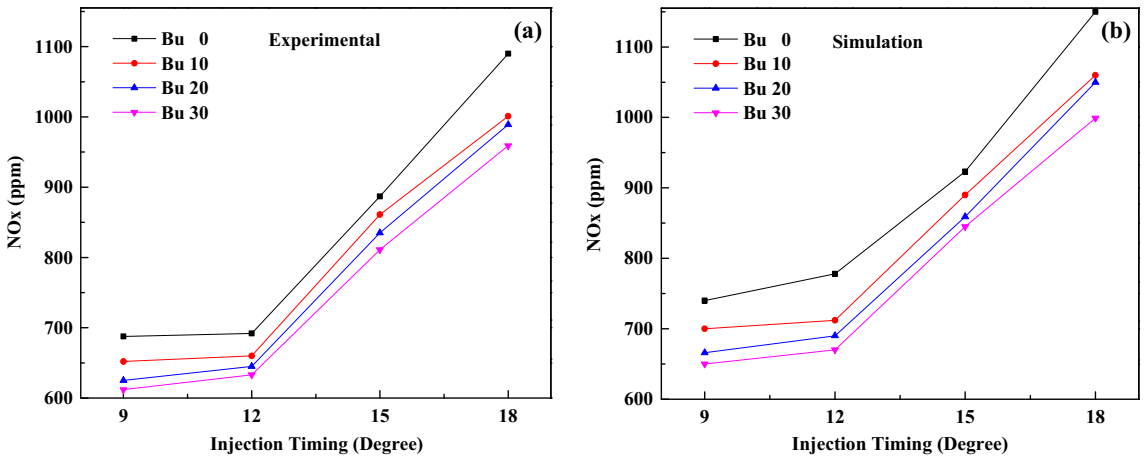

Fig. 9 Variation of NO_x versus injection timing. **a** Experimental. **b** Simulation

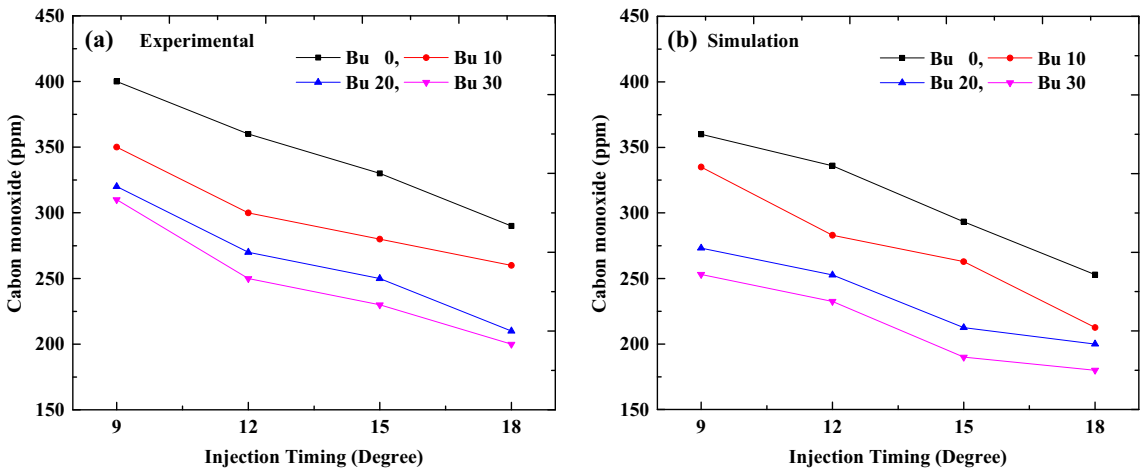

Fig. 10 Variation of CO versus injection timing. **a** Experimental. **b** Simulation

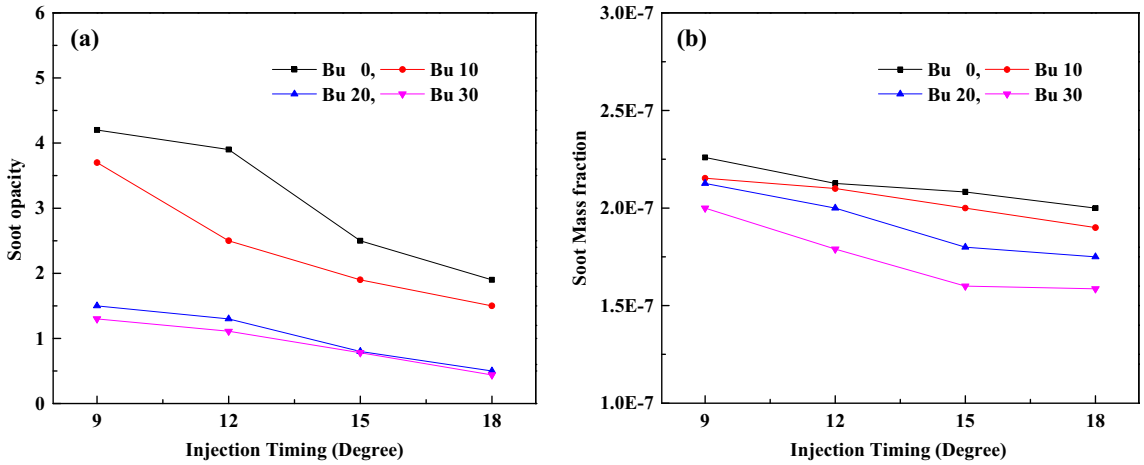

Fig. 11 Variation of soot opacity versus injection timing. **a** Experimental. **b** Simulation

results are obtained for soot mass fraction, and similar trend as compared to experimental results is observed.

Conclusion

In the present study, experimental and numerical investigations are carried out to determine the effects of butanol-diesel blend ratio and injection timing on the performance, combustion, and exhaust emission characteristics of CRDI engine. Based on obtained results, following conclusions are made:

- Peak in-cylinder pressure is marginally increased for n-butanol-diesel blends compared to neat diesel.
- The BTE are increased by ~ 4.5, 6, and 8%, respectively, for Bu10, Bu20, and Bu30, respectively, compared to neat diesel.
- Optimum injection timings for maximum BTE are obtained for various butanol-diesel blends including neat diesel. Injection timing of 12° BTDC is found optimum for neat diesel, whereas IT of 15° BTDC is found optimum for Bu10, Bu20, and Bu30.
- NO_x emissions are reduced with increasing n-butanol-diesel blends. The maximum NO_x emission is 1090, 1001, 989, and 959 ppm for Bu0, Bu10, Bu20, and Bu30 obtained experimentally at 18° BTDC, respectively.
- Increasing butanol content in the blends results in enhanced oxidation leads to reduction of soot and CO due to higher oxygen/carbon ratio.
- Results obtained from CFD study are showing good agreement with experimental data, which validate the proposed model for further investigations.

Acknowledgements The authors like to acknowledge AVL-AST, Graz, Austria, for the granted use of AVL-FIRE under the University Partnership Program.

References

Atmanli A, Ileri E, Yuksel B, Yilmaz N (2015) Extensive analyses of diesel–vegetable oil–n-butanol ternary blends in a diesel engine. Appl Energy 145:155–162

Campos-Fernández J, Arnal JM, Gómez J, Dorado MP (2012) A comparison of performance of higher alcohols/diesel fuel blends in a diesel engine. Appl Energy 95:267–275

Chen Z, Liu J, Han Z, Du B, Liu Y, Lee C (2013) Study on performance and emissions of a passenger-car diesel engine fueled with butanol–diesel blends. Energy 55:638–646

Chen Z, Wu Z, Liu J, Lee C (2014) Combustion and emissions characteristics of high n-butanol/diesel ratio blend in a heavy-duty diesel engine and EGR impact. Energy Convers Manag 78:787–795

Choi B, Jiang X, Kim YK, Jung G, Lee C, Choi I, Song CS (2015) Effect of diesel fuel blend with n-butanol on the emission of a turbocharged common rail direct injection diesel engine. Appl Energy 146:20–28

Chotwichien A, Luengnaruemitchai A, Jai-In S (2009) Utilization of palm oil alkyl esters as an additive in ethanol–diesel and butanol–diesel blends. Fuel 88(9):1618–1624

Colin O, Benkenida A (2004) The 3-zones extended coherent flame model (ECFM3Z) for computing premixed/diffusion combustion. Oil Gas Sci Technol 59(6):593–609

Dernotte J, Mounaim-Rousselle C, Halter F, Seers P (2010) Evaluation of butanol–gasoline blends in a port fuel-injection, spark-ignition engine. Oil Gas Sci Technol Rev Inst Fr Pétrol 65(2):345–351

Doğan O (2011) The influence of n-butanol/diesel fuel blends utilization on a small diesel engine performance and emissions. Fuel 90(7): 2467–2472

FIRE v2011 Manuals 2011 Graz. AVL LIST GmbH, Austria

Hansen AC, Taylor AB, Lyne PWL, Meiring P (1989) Heat release in the compression-ignition combustion of ethanol. Trans ASAE 32(5): 1507–1511

Heywood John (1988) Internal combustion engine fundamentals. McGraw-Hill Education, New York

Hulwan DB, Joshi SV (2011) Performance, emission and combustion characteristic of a multicylinder DI diesel engine running on diesel–ethanol–biodiesel blends of high ethanol content. Appl Energy 88(12):5042–5055

Ibrahim A (2016) Performance and combustion characteristics of a diesel engine fuelled by butanol–biodiesel–diesel blends. Appl Therm Eng 103:651–659

Jin C, Yao M, Liu H, Chia-fon FL, Ji J (2011) Progress in the production and application of n-butanol as a biofuel. Renew Sust Energ Rev 15(8):4080–4106

Kumar BR, Saravanan S (2016) Effects of iso-butanol/diesel and n-pentanol/diesel blends on performance and emissions of a DI diesel engine under premixed LTC (low temperature combustion) mode. Fuel 170:49–59

Kuo KK (1986) Principles of combustion. Wiley, India

Lamani VT, Yadav AK, Kumar GN (2017a) Effect of exhaust gas recirculation rate on performance, emission and combustion characteristics of common rail diesel engine fuelled with n-butanol-diesel blends. Biofuels. http://dx.doi.org/10.1080/17597269.2017.1369631

Lamani VT, Yadav AK, Narayanappa KG (2017b) Influence of low-temperature combustion and dimethyl ether-diesel blends on performance, combustion, and emission characteristics of common rail diesel engine: a CFD study. Environ Sci Pollut Res 24:15500–15509

Miers SA, Carlson RW, McConnell SS, Ng HK, Wallner T, Esper J L (2008) Drive cycle analysis of butanol/diesel blends in a light-duty vehicle (no. 2008-01-2381) SAE technical paper

Petranovic Z, Vujanovic M, Duic N (2015) Towards a more sustainable transport sector by numerically simulating fuel spray and pollutant formation in diesel engines. J Clean Prod 88:272–279

Rakopoulos DC, Rakopoulos CD, Giakoumis EG, Dimaratos AM, Kyritsis DC (2010a) Effects of butanol–diesel fuel blends on the performance and emissions of a high-speed DI diesel engine. Energy Convers Manag 51(10):1989–1997

Rakopoulos DC, Rakopoulos CD, Hountalas DT, Kakaras EC, Giakoumis EG, Papagiannakis RG (2010b) Investigation of the performance and emissions of bus engine operating on butanol/diesel fuel blends. Fuel 89(10):2781–2790

Rakopoulos DC, Rakopoulos CD, Papagiannakis RG, Kyritsis DC (2011) Combustion heat release analysis of ethanol or n-butanol diesel fuel blends in heavy-duty DI diesel engine. Fuel 90(5):1855–1867

Sarathy SM, Thomson MJ, Togbe C, Dagaut P, Halter F, Mounaim-Rousselle C (2009) An experimental and kinetic modeling study of n-butanol combustion. Combust Flame 156(4):852–864

Sayin C (2010) Engine performance and exhaust gas emissions of methanol and ethanol–diesel blends. Fuel 89(11):3410–3415

Sayin C, Uslu K, Canakci M (2008) Influence of injection timing on the exhaust emissions of a dual-fuel CI engine. Renew Energy 33(6):1314–1323

Schobert HH (2013) The chemistry of hydrocarbon fuels. Butterworth-Heinemann, Oxford

da Silva Trindade WR, dos Santos RG (2017) Review on the characteristics of butanol, its production and use as fuel in internal combustion engines. Renew Sust Energ Rev 69:642–651

Siwale L, Kristóf L, Adam T, Bereczky A, Mbarawa M, Penninger A, Kolesnikov A (2013) Combustion and emission characteristics of n-butanol/diesel fuel blend in a turbo-charged compression ignition engine. Fuel 107:409–418

Zhang ZH, Balasubramanian R (2014) Influence of butanol–diesel blends on particulate emissions of a non-road diesel engine. Fuel 118:130–136

Zhang Q, Yao M, Zheng Z, Liu H, Xu J (2012) Experimental study of n-butanol addition on performance and emissions with diesel low temperature combustion. Energy 47(1):515–521